Comparison of two contact detection methods for ground reaction forces and moment estimation during sidestep cuts, runs and walks

Pauline Morin, Antoine Muller, Georges Dumont, Charles Pontonnier

Pauline Morin
IRISA - UMR 6074,
Univ Rennes,
35000 Rennes,
France
email: pauline.morin@ens-rennes.fr

Antoine Muller
LBMC UMR T 9406,
Univ Lyon, Univ Gustave Eiffel, Univ Claude Bernard Lyon 1,
69000 Lyon,
France
email: antoine.muller@univ-lyon1.fr

Georges Dumont
IRISA - UMR 6074,
Univ Rennes,
35000 Rennes,
France
email: georges.dumont@ens-rennes.fr

Charles Pontonnier[1]
IRISA - UMR 6074,
Univ Rennes,
35000 Rennes,
France
email: charles.pontonnier@ens-rennes.fr

Comparison of two contact detection methods for ground reaction forces and moment estimation during sidestep cuts, runs and walks

Force plateforms often limit the analysis of human movement to the laboratory. Promising methods for estimating ground reaction forces and moments can overcome this limitation. The most effective family of methods consists of minimizing a cost, constrained by the subject's dynamic equilibrium, for distributing the force over the contact surface on the ground. The detection of contact surfaces over time is dependent on numerous parameters. This study proposes to evaluate two contact detection methods: the first based on foot kinematics and the second on pressure sole data. Optimal parameters for these two methods were identified for walking, running and sidestep cuts tasks. The results show that a single threshold in position or velocity is sufficient to guarantee a good estimate. Using pressure sole data to detect contact improves the estimation of the position of the centre of pressure. Both methods demonstrated a similar level of accuracy in estimating ground reaction forces.

Keywords: Biomechanics, Motion analysis, Ground reaction forces, Outside laboratory experiments

1 Introduction

Methods for analysing human movement based on inverse dynamics make it possible to calculate biomechanical quantities such as intersegmental moments during movement. They require ground reaction forces and moments (GRF&M), traditionally measured by force platforms. The analysis of human movement without the need for force platforms represents a major application opportunity outside the laboratory, with applications in many fields, such as sport, ergonomics and physical activity monitoring, requiring to estimate the GRF&M instead of measuring them.

Several approaches can be used to estimate GRF&M from motion capture data [1–3] or pressure insoles data [4, 5]. The estimation of GRF&M from motion capture data based on the equations of dynamics is indeterminate in the case of multiple contacts. Solving this indeterminacy using an optimization approach has already yielded good results on several movements and subjects [1, 6, 7]. A cost function is minimized, constrained by the subject's dynamic equilibrium to distribute the overall force over the contact surfaces.

In [1, 8, 9], contact surfaces are discretized into a set of points located under the feet (from 12 to 40 points under each foot). A point is considered to be in contact with the ground if its vertical position is lower than a position threshold z_0 (from 0.02 m to 0.04 m) and if its velocity norm is lower than a velocity threshold v_0 (from 0.8 m.s^{-1} to 1.3 m.s^{-1}). The position and velocity thresholds will hereafter be grouped together under the term kinematic thresholds. In [1], the kinematic thresholds ($z_0 = 0.03$ m and $v_0 = 0.8$ m.s^{-1}) were chosen using a preliminary sensitivity study on walking trials. In [8, 9], the values of the kinematic thresholds were defined empirically. The use of these kinematic thresholds is only possible for movement on a ground of known level. The adjustment of kinematic threshold values can be time-consuming and requires knowledge of motion analysis (order of magnitude of motion-specific velocities, errors in estimating positions from motion data), which is why the values presented are widely used without individualisation or adaptation to the task studied. In addition, the methods used in these studies consider a single-solid foot model. A two-solids foot model would a priori allow more accurate kinematic tracking and therefore better detection of contact via the use of kinematic thresholds.

Pressure insoles provide quantities (position of the centre of pressure, quantity of pressure on several zones under the feet) to describe foot-ground contact at the cost of a limited impact on the subject's movement [4, 5]. To our knowledge, no method based on an optimization approach for estimating the GRF&M uses the pressure sole data for contact detection. This type of pressure insole approach would be compatible with experiments outside the laboratory, allowing a wide range of application studies.

In the present study, two methods of estimating GRF&M differing in their method of contact detection were compared: one method of contact detection based on motion data and another based on pressure insole data. The performance of the methods was evaluated in terms of the accuracy of the GRF&M estimate relative to the force-platform data. This study assumes that by improving the contact detection method, the GRF&M estimation method will be improved. The first contact detection method was similar to that presented in the [1, 6, 9, 10] studies and used kinematic thresholds (position and velocity). The second was based on the use of pressure insoles using a pressure threshold. A parametric study was carried out to determine the thresholds for each of the two contact detection methods.

2 Material and methods

2.1 Experimental procedure. The cohort consisted of 4 women and 10 men (age: 29 ± 2 yo, height: 1.8 ± 0.1 m, weight: 70 ± 10 kg). The inclusion criterion was to wear size 38, 39, 42 or 43 shoes since two sizes of insoles were available (38-39

[1]Corresponding Author.
Version 1.18, October 24, 2023

and 42-43 EU). Each subject signed an informed consent form and a pseudonimisation protocol was followed for data storage. The experimental protocol was approved by INRIA's National Ethics Committee (Comité Opérationnel d'Evaluation des Risques Légaux et Ethiques, 2021-06, 22/02/2021).

Whole-body motion capture was performed by placing 46 reflective markers on standardised anatomical landmarks in accordance with the recommendations of the International Society of Biomechanics [11, 12]. Motion capture data were recorded using a Qualisys optoelectronic motion capture system (200 Hz, 22 12 Mpixels OQUS 7+ cameras). GRF&M were recorded with two AMTI force platforms (2000 Hz). The pressure under the foot, the position of the centre of pressure (CoP), the vertical force and the acceleration of the foot were recorded by Moticon® insoles (OpenGo, 100 Hz, 16 pressure cells covering 65% of the surface of the insole, with a resolution of $0.25 N/cm^2$ and a hysteresis of $< 1\%$ [13], an inertial measurement unit (IMU) at the centre of each insole). The insole data was linearly interpolated from 100 Hz to 200 Hz to match the frequency of the Qualisys system and synchronized with the optoelectronic data in accordance with [14]. The wireless insoles were inserted into the subjects' personal sports shoes.

Prior to data collection, the pressure insoles were reset and calibrated according to the manufacturer's recommendations. During the experiment, each subject performed 15 sidestep cuts, 15 runs and 15 walks at comfort speed, i.e. 15 trials per subject per condition to obtain an acceptable statistical comparison [15]. Sidestep cuts were always performed using the right foot as the support foot. Subjects had to modulate their stride so as not to touch the two platforms during a given step. Of the 630 trials collected, 521 trials were studied: the 45 trials relating to one participant that required additional pre-processing due to insole malfunction were discarded, as were 64 other trials for multiple causes (markers obscured, one-off pressure sole malfunction, platform data not usable due to failure to follow experimental instructions).

2.2 Contact detection. The area under each foot was divided into a set of 16 points. The points were defined on the foot model according to the coordinates of the centre of each pressure cell of the Moticon® insole: according to the manufacturer's documentation, the position of the centre of each pressure cell was defined in the reference frame of the sole and the position of the centre of each cell was expressed in the reference frame of the foot model. For this purpose, a transformation matrix between the sole frame and the foot frame, determined as in [14], was used. For all participants, the matrix used was that determined during a randomly selected running trial for the participant with the highest height, in order to obtain the most accurate placement of the contact points in relation to the foot. The points were located under the foot and the participants wore sports shoes (with sole thicknesses ranging from 0.01 m to 0.03 m). As a result, the vertical position of the points never reached zero.

Two contact detection methods were used to determine at each moment and for each contact point whether it was active, i.e. in contact with the ground.

The first method of contact detection was a kinematic threshold detection based on the method presented in [1, 6, 7, 9, 10]. Contact induced zero relative velocity between the foot and the ground (it was assumed that there was no sliding between the foot and the ground defined as a plane), which implied a constant distance that can be determined (minimum distance between the contact point and the ground). A point was considered active if its distance from the ground (corresponding to its vertical position if the ground was horizontal and to its normal given by the direction of gravity) was less than a threshold value z_0 and if the norm of its velocity was less than a threshold value v_0. A parametric study was carried out by comparing the results obtained with different threshold values:

- position threshold z_0 (in m) : 0.01 (minimum thickness of the shoe soles), 0.02, 0.05 [1], 0.1, 0.2 and 1;
- velocity threshold v_0 (in $\mathrm{m.s^{-1}}$) : 0.5, 0.8 [1], 3, 5 and 10.

The positions and velocities of the contact points were calculated from the trajectories of the markers and an osteo-articular model, in an inverse kinematics step. The human body was modelled by a geometric model composed of 19 rigid bodies linked by 17 joints corresponding to 43 degrees of freedom. A two-part foot model was chosen in order to better track the kinematics of the foot. The geometric model was calibrated using the method presented in [16]. The inverse kinematics step was performed using a multibody kinematics optimization performed with a penalty-based Levenberg-Marquardt algorithm [17]. The position of the markers and the joint coordinates were filtered using a Butterworth low-pass filter with no phase shift and at cut-off frequencies of 10 Hz and 5 Hz respectively, as recommended in [9, 18]. From the joint coordinates obtained, the position of the potential contact points was calculated using a direct geometric model, and their velocity was obtained using second-order finite differentiation of position.

The second method of contact detection was a pressure threshold detection. A point was considered to be in contact if the pressure measured at this point by the Moticon® pressure insole was higher than a threshold value p_0. A parametric study was carried out by comparing the results obtained with different pressure threshold values (in $\mathrm{N.cm^{-2}}$): 0 (pressure insoles contact detection criterion), 0.25 (insole measurement resolution), 1.5, 2, 3, 4, 5, 6, 7, 9, 11 and 13.

A permanent contact condition was also considered to challenge the usefulness of contact detection methods in the external force estimation method.

2.3 GRF&M estimation. To compare the contact detection methods, a method for estimating the GRF&M using an optimization approach was developed. This method was based on the method presented in [9] (Figure 1 shows the general methodology). The method used as input the motion data, the geometric model and the inertial model (established from anthropometric tables from [19]) specific to the participant.

The inverse kinematics step and the contact detection step were detailed in the previous paragraph.

In the dynamic equilibrium calculation step, global external forces and moments were computed using the Recursive Newton-Euler Algorithm (RNEA). The moments were expressed at the origin of the pelvis.

The distribution of the global effort estimated the force $\mathbf{F_i}$ (vector 3×1) on each active contact point among the N = 32 potential contact points. The external force vector $\mathbf{F}$ (vector 3N×1) corresponded to the concatenation of the vectors $\mathbf{F_i}$. As soon as at least three contact points were considered active, there was an infinite number of solutions (6 equation, 9 unknown). At each instant, a sequential quadratic programming method determined $\mathbf{F_i} = (\mathrm{Fi^x\ Fi^y\ Fi^z})^\top$ by solving the following minimization problem:

$$\min_{\mathbf{F}} \sum_{\mathrm{i}=1}^{\mathrm{N}} \|\mathbf{F_i}\|^2 \tag{1}$$

such as $\begin{cases} \text{Dynamic equilibrium of the whole body,} \\ \forall i \in [\![1, \mathrm{N}]\!],\ \mathrm{Fi^x} < \mathrm{F^x_{i_{max}}},\ \mathrm{Fi^y} < \mathrm{F^y_{i_{max}}} \text{ et } \mathrm{Fi^z} < \mathrm{F^z_{i_{max}}}. \end{cases}$

The problem was constrained by the dynamic equilibrium and by the maximal effort $\mathbf{F_{imax}} = (\mathrm{F^x_{i_{max}}\ F^y_{i_{max}}\ F^z_{i_{max}}})^\top$ defined as admissible for each potential contact point i. $\mathbf{F_{imax}}$ was proportional to the weight of the participant (BW). As in the study [10], a frictional cone was considered defined by Coulomb's law with a friction coefficient $\mu = 0.5$. This approximation was used to linearize the constraint. With $\mathbf{z}$ as the normal to the contact surface, we had:

$$\mathbf{F_{imax}} = k_i \times \begin{pmatrix} \mu \\ \mu \\ 1 \end{pmatrix} . \tag{2}$$

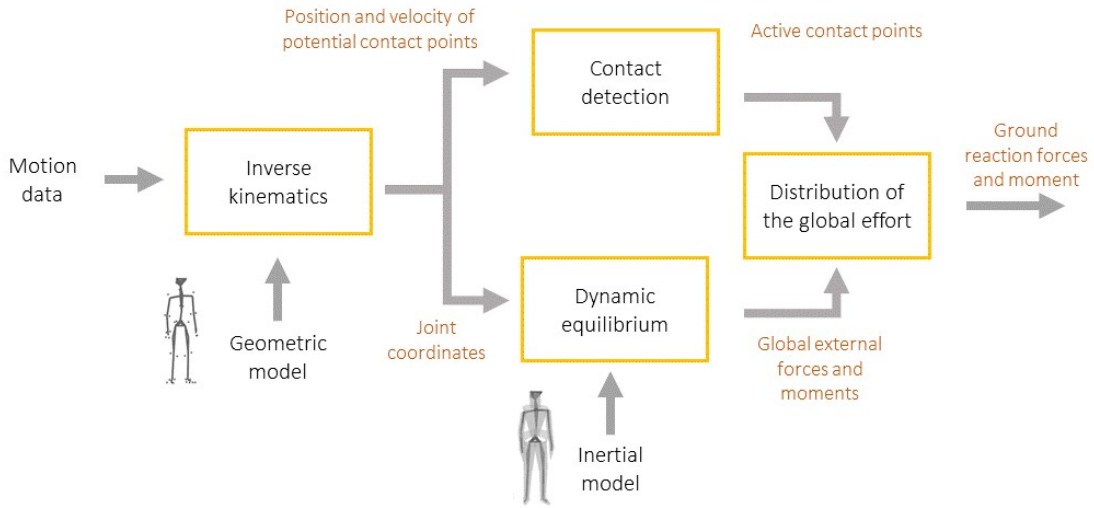

Fig. 1 **General methodology for estimating GRF&M from motion data based on the optimization approach. The different stages of the method are boxed in yellow. The quantities estimated during the method are shown in yellow. The input quantities (models and experimental data) are shown in black.**

The value of k_i depended on the number of active contact points:

$$k_i = \begin{cases} 0.4 \times \frac{\mathrm{N}}{\mathrm{N}_{active}(t)} \times \mathrm{BW} & \text{if the point is active,} \\ 0 & \text{else.} \end{cases} \quad (3)$$

The coefficient of 0.4 was determined empirically in [1, 9]. $\mathrm{N}_{active}(t)$ is the number of active contact points at time t, guaranteeing a constant reserve force at each instant.

Each component of the estimated effort was filtered using the same filter as that used to filter the joint coordinates in order to avoid the appearance of filtering artifacts [20]. All the methods were implemented in CusToM [21].

2.4 Parametric study. Both CoP position and resultant force were compared between measured and estimated data to assess the performance of a given set of contact detection parameters. Such comparison could only be done when at most one foot was in contact with a given force platform. Contact between the foot and the force platform was considered active when both measured and estimated forces were higher than 10 N [8, 22, 23] (the force platform admitted an accuracy of 0.5% of the measured force).

At each instant and for each foot, the error on the resultant force was defined as the norm of the difference between estimated $\mathbf{F_{estimated}}$ and measured $\mathbf{F_{pf}}$ resultant forces:

$$\mathrm{Error}_{\mathrm{resultant}} = \|\mathbf{F_{pf}} - \mathbf{F_{estimated}}\|. \quad (4)$$

At each instant and for each foot, the CoP position error (of zero altitude) was defined as the distance between estimated $\mathbf{CoP_{estimated}}$ and measured $\mathbf{CoP_{pf}}$ CoP positions:

$$\mathrm{Error}_{\mathrm{CoP}} = \|\mathbf{CoP_{estimated}} - \mathbf{CoP_{pf}}\|. \quad (5)$$

The root mean square errors (RMSEs) of these errors were calculated for each trial to quantify the difference between the estimated and measured [24]. The average RMSEs on the resultant force and on the position of the CoP were compared for each type of movement studied according to the values of the contact detection parameters used.

For both contact detection methods, the set of parameters giving the most accurate estimate of the external force for all types of movement was identified. For each type of movement studied and for each type of error, the minimum mean value of the RMSE ($RMSE_{min}$) was identified. This value was multiplied by a coefficient $k_{threshold} > 1$ and the RMSE results below $k_{threshold} * RMSE_{min}$ were retained. The value of $k_{threshold}$ was increased (with an increment of 0.01) until a set of detection thresholds was common to each type of movement and each type of error.

2.5 Comparison. The two contact detection methods were compared in terms of the accuracy of the GRF&M estimate obtained with the optimal parameters of each method. For each contact detection method, the average duration of contact sequences (the time during which at least one point belonging to the foot was in contact with the ground) and the average number of active contact points per contact phase were calculated. The average duration of the sequences during which the force platforms measured a force greater than 10 N was calculated.

The significance of differences in the accuracy of the GRF&M estimate was statistically tested. The distribution of RMSEs obtained with each detection method was compared using a Wilcoxon test after rejecting the hypothesis of a normal distribution using a Shapiro-Wilk test.

3 Results

The results of the parametric study on the choice of kinematic thresholds are presented in Figure 2. The optimum value for the position threshold was $z_0 = 0.05$ m and the optimum value for the velocity threshold was $v_0 = 3$ m.s^{-1} with $k_{threshold} = 1.17$. The results of the parametric study on the choice of the pressure threshold are presented in Figure 3. The optimum value for the pressure threshold was $p_0 = 4$ N.cm^{-2} with $k_{threshold} = 1.06$.

The error on the resultant force and on the CoP position obtained for each movement is summarized in Table 1 using each contact detection method and using a permanent contact. Both contact detection methods ensured a similar accuracy in estimating resultant force, whereas the pressure threshold allowed a better estimate of the CoP position.

The accuracy of the external force estimation decreased when the detection thresholds did not detect all the contact instants (Figure 2), e.g. for $z_0 = 0.01$ m and $v_0 = 0.5$ m.s^{-1}. The accuracy of the external force estimation decreased when the detection thresholds allowed permanent detection of contact (Figure 3).

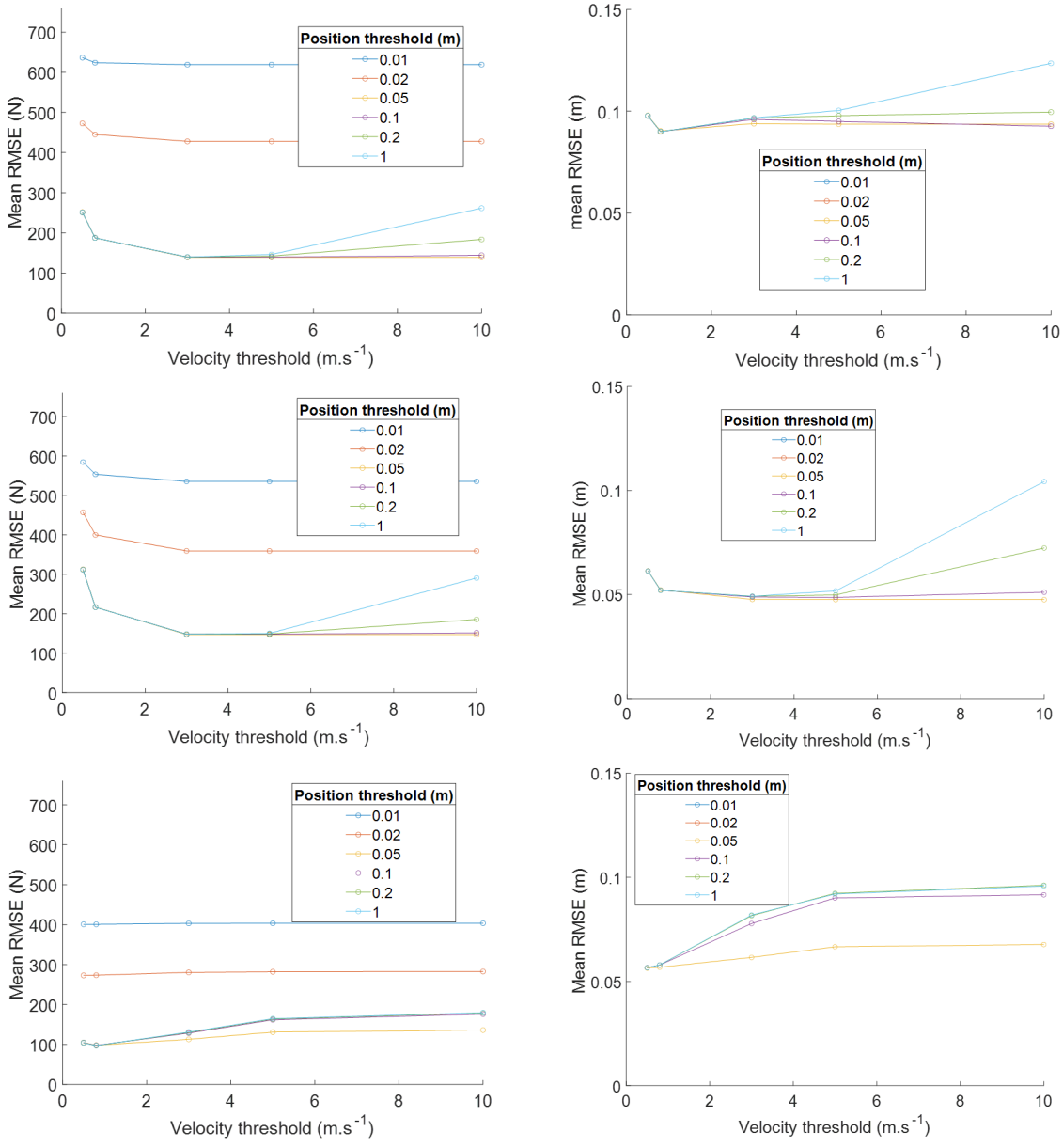

(*a*) Resultant force error

(*b*) CoP error

Fig. 2 Accuracy of the GRF&M estimate during sidestep cuts (top), runs (middle) and walks (bottom) according to the kinematic thresholds used: error on the resultant force and error on the CoP position.

The average contact times and the average number of active contact points during a contact are listed in Table 2 according to the type of motion. The absence of contact detection resulted in an null estimated external force and therefore a high error when the foot was actually in contact with the ground. The global equilibrium of the biomechanical model obtained from the RNEA algorithm generated dynamic residuals generated by kinematics and model innacuracies [25], in addition to the external forces. If a contact was detected unproperly, the method computed external forces to balance the residuals even if no actual force was measured.

The GRF&M were estimated for each trial using each contact detection method with the optimal parameter values. Component by component, the estimated GRF&M were compared to the GRF&M measured by the force platforms in Figure 4 (moments are expressed at the origin of the platforms).

The RMSEs obtained were normalized according to the mass of the participants for comparison with the literature in Table 3.

4 Discussion

The current study aimed at comparing two contact detection methods for GRF&M estimation. A parametric study was performed to find the best set of parameters to be used for the type of trials studied (walks. runs, and sidestep cuts).

4.1 Parametric study. The optimal values of the kinematic thresholds presented in [8] and [1] were $z_0 = 0.05$ m and $v_0 = 1$ m.s^{-1} for the study of various sports-related movements, and corresponded to the optimal values of the thresholds for the walking trials in our study. Sidestep cuts and runs involved more acceleration quantities than walking: the norm of the ground reaction force was significantly greater than the norm of the resultant of the forces corresponding to the action of gravity. The optimal value of the velocity threshold for these movements was logically higher than the optimal value of the velocity threshold for walking in our study.

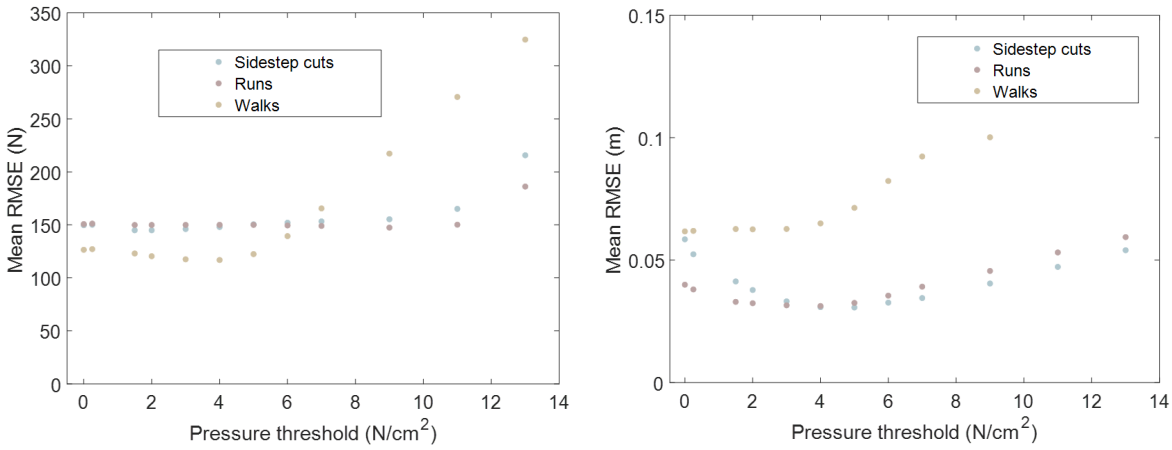

(*a*) Resultant force error (*b*) CoP error

Fig. 3 **Accuracy of the external force estimate according to the pressure threshold used.**

TABLE 1 **Resultant error and CoP position error for each movement and contact detection method.**

Contact detection method	Sidestep cut		Run		Walk	
Kinematic threshold (z_o=50mm et $v_0 = 3m.s^{-1}$)	94 mm	147 N	48 mm	144 N	62 mm	113 N
Pressure threshold ($p_0 = 4N.cm^{-2}$)	31 mm	148 N	31 mm	150 N	65 mm	117 N
Permanent contact	103 mm	264 N	95 mm	264 N	87 mm	177 N

4.2 Contact detection. In [22], the authors estimated the duration of the contact phases between 0.69 s and 1.00 s. Our study estimated the duration of contact phases for walking at 0.5 s. The difference may be explained by the elimination of the double stance phase at the end and/or beginning of the gait cycle if, in our study, it was performed with both feet on the same platform. The duration of certain contact phases did not correspond to complete contact phases of the gait and cannot be interpreted as such. They can however be compared according to the contact detection method. Differences in contact time for walk trials may also be explained by the stride modification of the subjects to avoid double contact phases on a single platform.

Sidestep cuts and runs are more dynamic movements than walking, with shorter contact times. The average contact duration for running (0.25 s with kinematic threshold detection and 0.24 s with pressure threshold detection) was comparable to the durations estimated in [26]: the authors estimated the average duration of contact phases during the runs at 0.25 s using a contact detection method based on thresholds on vertical force measured by a force platform.

In [23], contrary to our results, the authors described a significant difference between their results obtained from insole data and the use of kinematic thresholds for event detection during walks. This difference can be explained by the fact that the authors exploited the number of active pressure cells in the pressure insole to detect the contact instants.

Both contact detection methods detected similar contact durations (Table 2), but the kinematic threshold method detected contact over the entire foot, in a more global way than the pressure threshold method, which detected contact with more finesse locally. This phenomenon can be seen in Figure 5 where there was two alternatives phases for the contact detection method with kinematic thresholds : a phase with zero contact points detected as active, and a phase where all the points under the foot are detected as active. For the pressure threshold contact detection method, there was a phase with zero contact points and a phase with a fluctuating number of active contact points. Walking is characterized by the foot rolling over the ground, which the kinematic threshold detection method did not detect compared to the pressure threshold method. Such observation may militate to develop a more detailed model of the foot to test its capability to discriminate the contact zones of the foot during the gait with regard to the current method, or to individualize the kinematic thresholds per contact point.

4.3 Estimation accuracy. Considering the CoP position estimation accuracy, [8] estimated the mean RMSE to be 25 mm along the anteroposterior axis and 9 mm along the mediolateral axis for running and 23 mm along the anteroposterior axis and 9 mm along the mediolateral axis for walking. The difference with our results may be explained by different experimental conditions: in [8], participants moved on a treadmill which should affect the length of CoP trajectories along each axis.

Considering the GRF&M estimation accuracy, the differences in RMSE between the results obtained in our study and in [9] may be related to the difference in the movements studied: the movements in our study are more dynamic than manual handling tasks. We compared our results obtained in running with those in [8] obtained for movements at a speed of 3 m.s^{-1}; we compared our results in walks with those obtained for a movement at 1.4 m.s^{-1}. Our study did not include tasks comparable to the squat and step-up tasks studied in [1]. AP and ML components may also be affected by the lack of minimization of the internal forces during the motion [27].

4.4 Perspective of use. The search for optimal values for the kinematic thresholds common to all the movements studied necessitated a deterioration in the accuracy of the external force estimate compared with the minimum value obtained with another set of kinematic thresholds (for walk trials, the RMSE on the re-

Table 2 Average duration of contact phases and average number of active contact points during a contact phase according to the contact detection method and the movement studied.

	Contact duration (s)			Mean number of active contact points	
	Kinematic threshold	Pressure threshold	Plateforme	Kinematic threshold	Pressure threshold
Sidestep cut	0.28 ± 0.04	0.27 ± 0.04	0.28 ± 0.04	10.6 ± 1	8.1 ± 0.7
Run	0.25 ± 0.03	0.24 ± 0.03	0.24 ± 0.03	10.8 ± 1	8.5 ± 0.8
Walk	0.50 ± 0.06	0.48 ± 0.01	0.43 ± 0.03	11.4 ± 1	5.0 ± 0.7

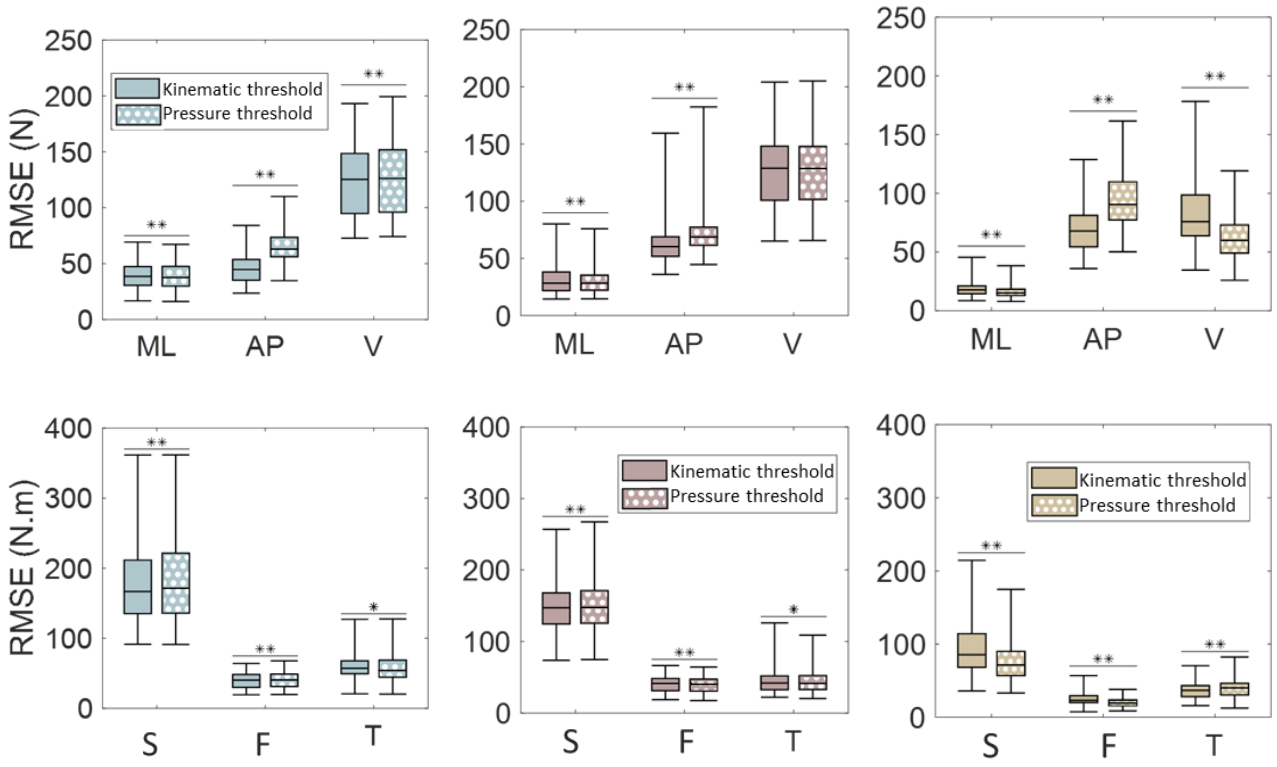

Fig. 4 RMSE between the estimated GRF&M and the GRF&M measured by the force platforms according to the contact detection method. The pattern in the boxes differentiates the contact detection method used. The RMSE for each component of the GRF&M is represented: the resultant along the medial-lateral axis (ML), along the anterior-posterior axis (AP), along the vertical axis (V) and the axis moment normal to the frontal plane (F), to the sagittal plane (S), to the transverse plane (T). Pairwise comparison (Wilcoxon) are indicated by "" for p < 0.001 and "*" for p < 0.01.**

sultant force was 13% higher than its minimum value). A position threshold of z_0 = 0.05 m and a velocity threshold greater than v_0 = 3 m.s^{-1} as well as a position threshold greater than z_0 = 0.05 m and a velocity threshold of v_0 = 3 m.s^{-1} make it possible to obtain an accuracy of estimation of the external error comparable to the accuracy obtained with the set of parameters z_0 = 0.05 m and v_0 = 3 m.s^{-1}. Contact detection can therefore be implemented using a single kinematic threshold, either in position or velocity. This result makes it possible to envisage other experimental conditions for contact detection, based on other technologies: for example, an inertial measurement unit (IMU) measures the acceleration of the foot over time and, by integration, the speed of the foot, which is sufficient in some cases to detect contact. By using a single position threshold, contact can be detected using distance sensors between the foot and the ground.

For the contact method using pressure threshold, the low value of $k_{threshold}$=1.06 suggested using a common pressure threshold for all the studied movements. The use of a single threshold means that tests involving different types of movement can be studied. The estimation of the external forces with pressure insoles can be implemented on mobile floors, of different heights to study the ascent of steps for example.

None of the contact detection methods consistently performed better on all GRF&M components. The pressure threshold contact detection method constrained the minimization problem more than the kinematic threshold method by systematically detecting fewer contact points during contact phases. This had no significant impact on the overall accuracy of the method. The use of sole data to detect contact allowed us to know more precisely which areas of the foot were in contact during movement. As a result, the error in estimating the position of the CoP was lower than with the kinematic threshold method. Nevertheless, the accuracy obtained in estimating the COP using a contact detection method based on a pressure threshold was inferior to estimating the position of the CoP based on its direct measurement by the insole [14].

4.5 Limitations and perspectives. The kinematic thresholds used were equal for all the contact points placed under the foot and therefore at different heights (effect linked to the shape of the shoes and soles). Each contact point had its own trajectory.

Table 3 Comparative table of RMSEs normalized by the weight of participants between external forces estimated and measured by force platforms according to different studies.

Reference	Motion	V (N/kg)	AP (N/kg)	ML (N/kg)
Kinematic thresholds	Sidestep cut	1.79	0.67	0.57
	Run	1.82	0.88	0.46
	Walk	1.15	0.98	0.26
Pressure threshold	Sidestep cut	1.80	0.94	0.55
	Run	1.81	1.02	0.44
	Walk	0.88	1.34	0.23
[1]	Walk	0.68	0.30	0.19
	Squat and step up	0.70	0.24	0.29
[8]	Walk	0.94	0.42	0.17
	Run	2.45	0.69	0.19
[9]	Handling task	0.51	0.22	0.19

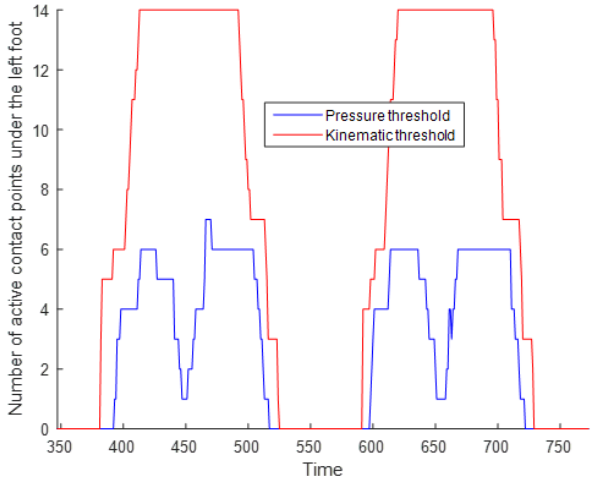

Fig. 5 Example of contact detection during a walking trial under the participant's left foot using the kinematic threshold (red) and pressure threshold (blue) contact detection method.

The relatively high value of $k_{threshold}$=1.17 for contact detection with kinematic thresholds suggests caution when using a unique set of kinematic thresholds for different types of movement. The comparison of the two contact detection methods can be envisaged with detection thresholds specific to each type of movement. The method with kinematic thresholds therefore requires a calibration phase (potentially specific to the movement, the participant, each contact point, etc.).

When the pressure threshold used exceeds a certain value (depending on the movement studied), the accuracy of the external force estimate decreases as the pressure threshold increases. This decrease was clearly identified for walking tests with a pressure greater than p_0 = 4 N.cm^{-2}. The pressure thresholds tested did not allow the same phenomenon to be observed for sidestep cuts and runs. Higher thresholds could complete the study. This study could include a study of the pressure measured over time in order to understand at which instants the values around p_0 = 4 N.cm^{-2} correspond.

If the estimated overall force is zero, as is the case during phases of flight, the estimated force under the feet must be zero. Detecting a greater number of contact points or detecting active contact points during phases of flight should not deteriorate the accuracy of the external force. The results of this study showed that taking into account a force with no contact condition (permanent contact) deteriorated the accuracy. A study of the dynamic residuals and the estimation error of the global external force could complete this study with regard to the kinematic results.

Each component of the external force on each solid (right foot, toes of the right foot, left foot and toes of the left foot) was filtered with a cut-off frequency of 5 Hz. According to [18], this cut-off frequency is suitable for studying human movement but degrades the information at the instants when contact begins and ends. The use of a filter with a higher cut-off frequency or an adaptive filter such as a Kalman filter could be considered. Other smoothing techniques can be used to improve the prediction results during these phases too [10].

5 Conclusion

Two contact detection methods were evaluated on different displacement movements. Contact detection can be based on the use of kinematic thresholds: contact is detected if the foot is close to the ground and not moving. This method can be used with just one of these two criteria, chosen according to the experimental constraints. Contact detection using pressure insoles data can be deployed outside the laboratory. The value of the threshold does not vary according to the movement studied: the study of sequences comprising different movements can be considered. Using insole data to detect contact provides a better estimate of the CoP compared to estimating the CoP with a contact detection method based on foot kinematics. The two contact detection methods demonstrated comparable accuracy in terms of estimating the magnitude of the external forces whereas exhibiting different accuracy component per component.

Acknowledgments

This study was partially supported by the ANR within the framework of the PIA EUR DIGISPORT project (ANR-18-EURE-0022). This work was partially supported by French government funding managed by the National Research Agency under the Investments for the Future program (PIA) with the grant ANR-21-ESRE-0030 (CONTINUUM project).

References

[1] Fluit, R., Andersen, M. S., Kolk, S., Verdonschot, N., and Koopman, H. F. J. M., 2014, "Prediction of ground reaction forces and moments during various activities of daily living," Journal of Biomechanics, **47**(10), pp. 2321–2329.

[2] Karatsidis, A., Bellusci, G., Schepers, M., de Zee, M., Andersen, M., and Veltink, P., 2017, "Estimation of Ground Reaction Forces and Moments During Gait Using Only Inertial Motion Capture," Sensors, **17**, p. 75.

[3] Oh, S. E., Choi, A., and Mun, J. H., 2013, "Prediction of ground reaction forces during gait based on kinematics and a neural network model," Journal of Biomechanics, **46**(14), pp. 2372–2380.

[4] Forner-Cordero, A., Koopman, H. J. F. M., and Helm, F. C. T. v. d., 2006, "Inverse dynamics calculations during gait with restricted ground reaction force information from pressure insoles," Gait & Posture, **23**(2), pp. 189–199.

[5] Honert, E. C., Hoitz, F., Blades, S., Nigg, S. R., and Nigg, B. M., 2022, "Estimating Running Ground Reaction Forces from Plantar Pressure during Graded Running," Sensors, **22**(9).

[6] Muller, A., Pontonnier, C., and Dumont, G., 2020b, "Motion-Based Prediction of Hands and Feet Contact Efforts During Asymmetric Handling Tasks," IEEE Transactions on Biomedical Engineering, **67**(2), pp. 344–352.

[7] Demestre, L., Morin, P., May, F., Bideau, N., Nicolas, G., Pontonnier, C., and Dumont, G., 2022, "Motion-Based Ground Reaction Forces and Moments Prediction Method for Interaction With a Moving and/or Non-Horizontal Structure," Journal of Biomechanical Engineering, **144**(11).

[8] Jung, Y., Jung, M., Ryu, J., Yoon, S., Park, S.-K., and Koo, S., 2016, "Dynamically adjustable foot-ground contact model to estimate ground reaction force during walking and running," Gait & Posture, **45**, pp. 62–68.

[9] Muller, A., Pontonnier, C., Robert-Lachaine, X., Dumont, G., and Plamondon, A., 2020a, "Motion-based prediction of external forces and moments and back loading during manual material handling tasks," Applied Ergonomics, **82**, p. 102935.

[10] Skals, S., Jung, M. K., Damsgaard, M., and Andersen, M. S., 2017, "Prediction of ground reaction forces and moments during sports-related movements," Multibody System Dynamics, **39**(3), pp. 175–195.

[11] Wu, G., Siegler, S., Allard, P., Kirtley, C., Leardini, A., Rosenbaum, D., Whittle, M., D'Lima, D. D., Cristofolini, L., Witte, H., Schmid, O., and Stokes, I., 2002, "ISB recommendation on definitions of joint coordinate system of various joints for the reporting of human joint motion–part I: ankle, hip, and spine. International Society of Biomechanics," Journal of Biomechanics, **35**(4), pp. 543–548.

[12] Wu, G., van der Helm, F. C. T., (DirkJan) Veeger, H. E. J., Makhsous, M., Van Roy, P., Anglin, C., Nagels, J., Karduna, A. R., McQuade, K., Wang, X., Werner, F. W., and Buchholz, B., 2005, "ISB recommendation on definitions of joint coordinate systems of various joints for the reporting of human joint motion—Part II: shoulder, elbow, wrist and hand," Journal of Biomechanics, **38**(5), pp. 981–992.

[13] "MoticonREGO AG. Sensor Insole Specification. Available online: https://moticon.com/wp-content/uploads/2021/09/OpenGo-Sensor-Insole-Specification-A4SQ-RGB-EN-03.02.pdf (consulté le 28 juin 2022)," .

[14] Morin, P., Muller, A., Pontonnier, C., and Dumont, G., 2022, "Evaluation of the Foot Center of Pressure Estimation from Pressure Insoles during Sidestep Cuts, Runs and Walks," Sensors, **22**(15).

[15] Forrester, S. E., 2015, "Selecting the number of trials in experimental biomechanics studies," International Biomechanics, **2**, pp. 62 – 72.

[16] Puchaud, P., Sauret, C., Muller, A., Bideau, N., Dumont, G., Pillet, H., and Pontonnier, C., 2020, "Accuracy and kinematics consistency of marker-based scaling approaches on a lower limb model: a comparative study with imagery data," Computer Methods in Biomechanics and Biomedical Engineering, **23**(3), pp. 114–125.

[17] Livet, C., Rouvier, T., Sauret, C., Pillet, H., Dumont, G., and Pontonnier, C., 2022, "A penalty method for constrained multibody kinematics optimisation using a Levenberg–Marquardt algorithm," Computer Methods in Biomechanics and Biomedical Engineering, pp. 1–12.

[18] Skogstad, S., Nymoen, K., Høvin, M., Holm, S., and Jensenius, A., 2013, *Filtering Motion Capture Data for Real-Time Applications*, graduate school of culture technology, kaist ed., Proceedings of the International Conference on New Interfaces for Musical Expression.

[19] Dumas, R., Chèze, L., and Verriest, J. P., 2007, "Adjustments to McConville et al. and Young et al. body segment inertial parameters," Journal of Biomechanics, **40**(3), pp. 543–553.

[20] Edwards, W. B., Derrick, T. R., and Hamill, J., 2017, "Time Series Analysis in Biomechanics," *Handbook of Human Motion*, B. Müller, S. I. Wolf, G.-P. Brueggemann, Z. Deng, A. McIntosh, F. Miller, and W. S. Selbie, eds., Springer International Publishing, Cham, pp. 1–24.

[21] Muller, A., Pontonnier, C., Puchaud, P., and Dumont, G., 2019, "CusToM: a Matlab toolbox for musculoskeletal simulation," Journal of Open Source Software, **4**(33), p. 927.

[22] Ghoussayni, S., Stevens, C., Durham, S., and Ewins, D., 2004, "Assessment and validation of a simple automated method for the detection of gait events and intervals," Gait & Posture, **20**(3), pp. 266–272.

[23] Catalfamo, P., Moser, D., Ghoussayni, S., and Ewins, D., 2008, "Detection of gait events using an F-Scan in-shoe pressure measurement system," Gait & Posture, **28**(3), pp. 420–426.

[24] Ren, L., Jones, R. K., and Howard, D., 2008, "Whole body inverse dynamics over a complete gait cycle based only on measured kinematics," Journal of Biomechanics, **41**(12), pp. 2750 – 2759.

[25] Muller, A., Pontonnier, C., and Dumont, G., 2017, "Uncertainty propagation in multibody human model dynamics," Multibody System Dynamics, **40**(2), pp. 177–192.

[26] Mo, S. and Chow, D. H. K., 2018, "Accuracy of three methods in gait event detection during overground running," Gait & Posture, **59**, pp. 93–98.

[27] Pontonnier, C., Livet, C., Muller, A., Sorel, A., Dumont, G., and Bideau, N., 2019, "Ground reaction forces and moments prediction of challenging motions: fencing lunges," Computer Methods in Biomechanics and Biomedical Engineering, **22**(sup1), pp. S523–S525.

List of Figures

List of Tables